# Neutron-diffraction study of the antiferromagnetic form factor of $La_2NiO_4$

Xun-Li Wang, C. Stassis, D. C. Johnston, T. C. Leung, J. Ye, and B. N. Harmon
*Ames Laboratory and Department of Physics, Iowa State University, Ames, Iowa 50011*

G. H. Lander
*Commission of European Communities, Joint Research Center, Postfach 2340, D-7500 Karlsruhe, Federal Republic of Germany*

A. J. Schultz and C.-K. Loong
*Argonne National Laboratory, Argonne, Illinois 60439*

J. M. Honig
*Department of Chemistry, Purdue University, West Lafayette, Indiana 47907*
(Received 18 July 1991; revised manuscript received 23 January 1992)

Neutron-diffraction techniques have been used to study the antiferromagnetic form factor of a $La_2NiO_4$ single crystal at 15 K. The antiferromagnetic form factor was obtained by measuring the integrated intensities of 16 magnetic reflections. A plateau is clearly seen at low $Q$ (up to 3 $Å^{-1}$) in the experimentally determined form factor, similar to those observed for $La_2CuO_4$ and $Sr_2CuO_2Cl_2$. The magnetization density deduced from the experimental data exhibits strong ansiotropy in the Ni-O plane. The experimental data are compared with covalency models and a recent spin-polarized band calculation.

## I. INTRODUCTION

Over the past few years, the magnetic properties of high-$T_c$ superconductors have been the central focus of many experimental investigations. Among these extensively studied compounds, $La_2CuO_4$, which has a $K_2NiF_4$ crystal structure, has received special attention. Neutron inelastic-scattering experiments[1] have established that the spin dynamics in this compound is similar to that of a two-dimensional (2D) spin-$\frac{1}{2}$ Heisenberg antiferromagnet. Considerably less is known about the electronic structure of the antiferromagnetic ground state. Of particular interest in this respect is information about the magnetization density of the ordered state, which can be obtained through a Fourier transform of the magnetic form factor measured by neutron scattering. An early neutron-diffraction experiment by Freltoft *et al.*[2] shows that the antiferromagnetic form factor of $La_2CuO_4$ exhibits a plateau in the low-$Q$ region (where **Q** is the neutron-scattering vector), and as a result, it cannot be fitted satisfactorily to a $Cu^{2+}$ ionic form factor. Similar results were reported[3] for $Sr_2CuO_2Cl_2$, a compound in which the out-of-plane oxygen atoms are replaced by Cl atoms. This similarity suggests that the main characteristics of the antiferromagnetic form factors of these compounds are related to the Cu-O planes, a common feature of their structures. In both cases the antiferromagnetic moments[2-4] on the $Cu^{2+}$ ions were found to be between $0.4\mu_B$ and $0.6\mu_B$. Since the magnetic structure factor is proportional to the square of the magnetic moment, this relatively small moment per Cu atom limits the precision attainable in studies of the cuprates. A much more favorable situation exists for the Ni compounds, where a theoretical maximum of $2\mu_B$ per Ni atom is expected. We are motivated, therefore, to undertake a systematic neutron-diffraction study of the antiferromagnetic form factor of $La_2NiO_4$, a compound which in many aspects closely resembles $La_2CuO_4$. A brief report of this work has been published[5] elsewhere. In the present paper, we present a detailed account of these experiments.

## II. EXPERIMENTAL DETAILS

$La_2NiO_4$ exhibits a structural distortion at $\sim$650 K from the high-temperature tetragonal (HTT) phase, with space group $I4/mmm$, to the low-temperature orthorhombic (LTO) phase, with space group $Bmab$. Another transition[6,7] to a lower-symmetry low-temperature tetragonal (LTT) phase, with space group $P4_2/ncm$, takes place at $\sim$70 K. The crystal structure parameters at 10 K have been refined and are given in Ref. 7.

Stoichiometric $La_2NiO_4$ orders antiferromagnetically[8] with $T_N \sim 650$ K. The magnetic structure in the LTO phase has been well established[9] by both unpolarized and polarized neutron experiments: The spins and magnetic propagation wave vector are parallel to the [1 0 0] direction.

Our measurements were conducted at 15 K, i.e., with the compound in the LTT phase. Based on the previously reported observation that there is no change in the intensity of the (0 1 1) magnetic reflection through the transition temperature ($\sim$70 K), it was argued[6,7] that the magnetic structure remains unchanged at the LTO-LTT transition. To verify this, we measured the temperature dependence of the (0 1 1) and (0 3 3) magnetic reflections and found no evidence of any change in their intensities

 

around 70 K. It should be pointed out, however, that these results do not rule out[6,7,10] the possibility of a more complicated double-**k** magnetic structure. However our analysis of the magnetization density does not depend on whether we have a single- or multiple-**k** structure. In the former case, we measure the total magnetization density; in the latter, we measure a particular component only. Assuming a single-**k** magnetic structure, there will be two equally populated magnetic domains with spins parallel to [1 0 0] and [0 1 0], respectively, because of the tetragonal symmetry in the LTT phase. Under the same assumption, it is easy to show that only magnetic reflections ($hkl$) with $h+k=$odd are allowed. Reliable measurements of the magnetic intensities can be obtained for the (0,odd,odd) and (odd,even,0) type of reflections, since the nuclear structure factors of these reflections are zero in the LTT crystal structure.

The neutron-diffraction experiments were performed at the Intense Pulsed Neutron Source of Argonne National Laboratory using a time-of-flight single-crystal diffractometer (SCD) equipped with a large-area ($30\times30$ cm$^2$) position-sensitive detector. Detailed measurements of the antiferromagnetic intensities were performed on a small crystal (of approximate dimensions $1.5\times1.5\times4.0$ mm$^3$) extracted from a larger specimen previously studied in Ref. 7. The crystal was mounted on the cold block of a closed-cycle He refrigerator installed on the sample table of the diffractometer, and it was kept at 15 K.

The time-of-flight spectrometer used in the experiment has three distinct advantages over diffractometers at steady-state reactors. First, because of the white incident beam used here, many diffraction peaks within a large volume of reciprocal space can be measured simultaneously with the crystal held at a fixed orientation. To demonstrate this, we show in Fig. 1 the diffraction pattern of ($0\,k\,l$) reflections measured at one crystal setting. Second, by rotating the crystal, one can measure the same diffraction peak over a wide range of neutron wavelengths. As will be discussed below, this capability is very useful in assessing the possible contamination of the data by multiple Bragg scattering, which is not negligible in these experiments. Finally, there is no contamination due to the high-order reflections.

The antiferromagnetic form factors of $La_2NiO_4$ were derived from the integrated intensities of several magnetic Bragg reflections. The measured integrated intensities, corrected for sample absorption, the detector efficiency, dead-time loss, and the incident neutron spectrum, are proportional to the magnetic structure factor. To determine the scale factor, we fitted the corrected integrated intensities of a selected number of nuclear reflections to the nuclear structure factors evaluated using the structure parameters in Ref. 7. In Fig. 2 and Table I, the normalized integrated intensities of these reflections are compared to the calculated nuclear structure factors. In this normalization procedure, only weak nuclear reflections and reflections with moderate nuclear structure factors, but measured at relatively short wavelengths, were included. This procedure was adopted in order to minimize the effect of the uncertainties in the extinction correction of the nuclear intensities.

Special attention was given to possible contamination of the data from multiple Bragg scattering. This is important because the magnetic intensities in $La_2NiO_4$ are weak compared to the nuclear ones and, as a result, can be strongly influenced by multiple Bragg scattering.

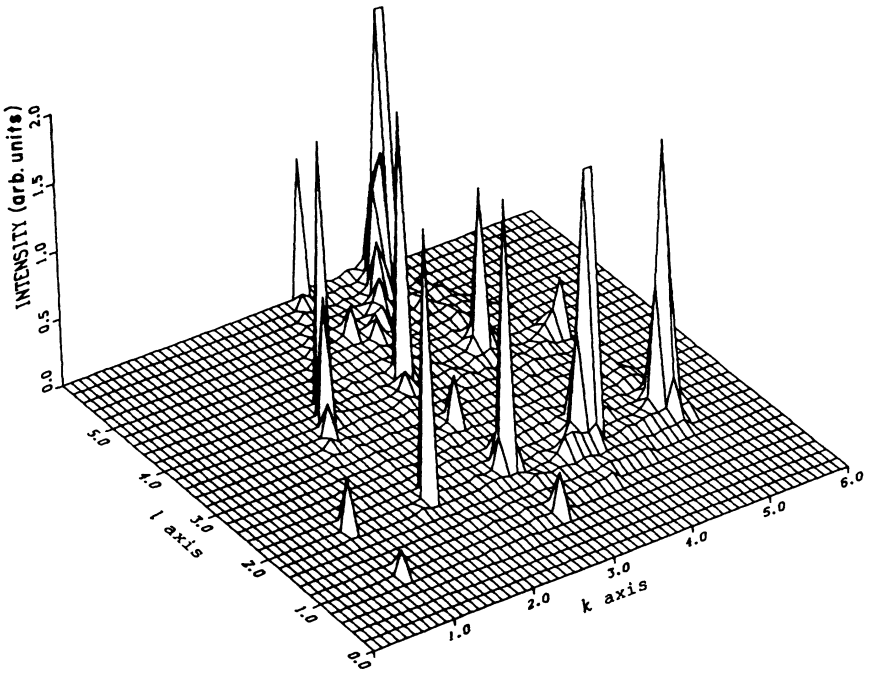


FIG. 1. Diffraction pattern of the $La_2NiO_4$ ($0\,k\,l$) plane as measured with the IPNS single-crystal diffractometer. Note that (0 1 1), (0 3 1), (0 3 3), and (0 3 5) are purely magnetic reflections. The intensity is in arbitrary units. The strong nuclear reflections have been truncated to promote the visibility of the weak magnetic reflections.

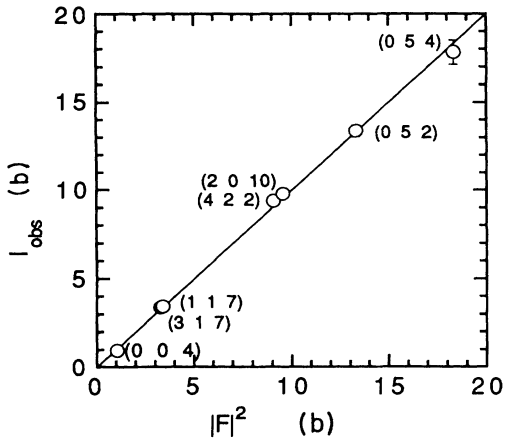


FIG. 2. Normalized integrated intensity $I_{obs}$ vs the calculated structure factor $|F|^2$ for a number of nuclear reflections used in the normalization procedure (see text).

Multiple Bragg scattering occurs when more than one reciprocal lattice point lies on the Ewald sphere and results in an anomalous Bragg reflection intensity for a given neutron wavelength and a particular crystal orientation. In the experiment each reflection is repeatedly measured over a large range of neutron wavelengths. The measurements that may have been contaminated by multiple Bragg scattering were identified by examining the wavelength dependence of each magnetic reflection. We illustrate the procedure by reference to Fig. 3. Figure 3(a) shows the intensity of the {3 1 1} nuclear reflections as measured at various wavelengths. It can be seen that six of these measurements may have been contaminated by multiple Bragg scattering, while the remaining eight measurements are consistent among themselves and are in agreement with the calculated value, which is represented by the dashed line. Figure 3(b) illustrates the application of this procedure to the measurements of the (0 1 9) magnetic reflection; measurements that may be contaminated by multiple Bragg scattering were discarded and the average of the remaining consistent set of data [dashed line in Fig. 3(b)] was taken as representing the magnetic structure factor for this reflection. This procedure was applied to each of the magnetic reflections, as well as the

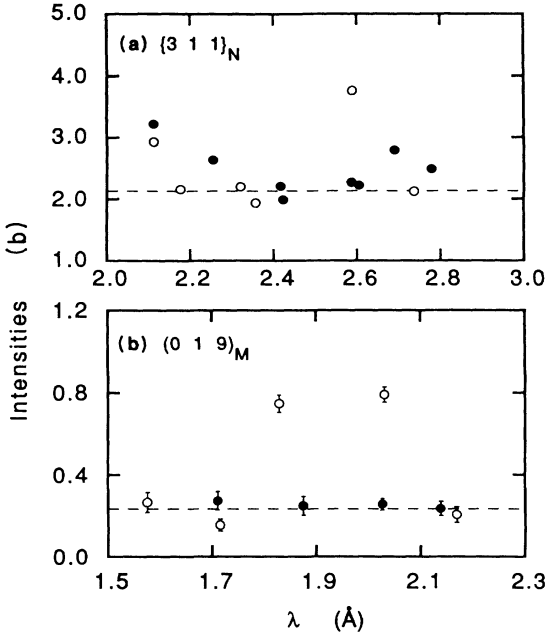


FIG. 3. Wavelength dependence of the observed intensities to demonstrate the multiple Bragg scattering effects. (a) {3 1 1} nuclear reflections. Open circles, (31−1); solid circles, (311). The dashed line is the calculated value. (b) (0 1 9) magnetic reflection. Solid and open circles correspond to different scans. The dashed line is the average of seven self-consistent data points.

nuclear reflections used in the normalization process.

To estimate the extinction correction, we used the extinction parameter previously determined for this crystal in Ref. 7. The extinction effects were found to introduce only minor adjustments to the data: a maximum of 10% for the (0 1 1) reflection and much smaller effects for the other reflections.

The quantity $\mu f(\mathbf{Q})$, where $\mu$ is the averaged ordered moment per Ni atom and $f(\mathbf{Q})$ the normalized magnetic form factor, is proportional to the magnetic scattering amplitude; for a colinear antiferromagnet, it is related to the magnetic structure factor by the equation

$$F = p\langle q\rangle \sum_d \sigma_d \exp(i\mathbf{Q}\cdot\mathbf{r}_d)e^{-W} . \quad (1)$$

TABLE I. Normalized integrated intensities as compared to the calculated structure factors for the nuclear reflections used in the normalization procedure (see text).

| ($h$ $k$ $l$) | Number of measurements | Neutron wavelengths λ (Å) | Normalized integrated intensities (b) | Calculated structure factor (b) |
|---|---|---|---|---|
| (004) | 4 | 3.95–4.61 | 0.95±0.03 | 1.04 |
| (317) | 3 | 1.70–2.02 | 3.39±0.25 | 3.28 |
| (117) | 4 | 2.00–2.60 | 3.44±0.19 | 3.39 |
| (422) | 4 | 1.62–1.93 | 9.40±0.24 | 9.07 |
| (2010) | 4 | 1.61–1.79 | 9.79±0.15 | 9.54 |
| (052)[a] | 5 | 1.27–1.70 | 13.18±0.33 | 13.32 |
| (054)[a] | 3 | 1.63–1.67 | 17.84±0.68 | 18.32 |

[a]These two reflections are also allowed by the magnetic structure. However, the intensities due to magnetic scattering are estimated less than 0.15 barn (see below), and, as a result, are insignificant considering the relatively large error bars of the observed structure factor.

TABLE II. Neutron-diffraction results of $La_2NiO_4$, at 15 K, for 16 magnetic reflections.

| ($h$ $k$ $l$) | $\sin\theta/\lambda$ (Å$^{-1}$) | Number of measurements | Neutron wavelenghts $\lambda$ (Å) | Insensities (b) | $\langle q\rangle^2$ | $\mu f(\mathbf{Q})$ ($\mu_B$) |
|---|---|---|---|---|---|---|
| (0 1 1) | 0.0993 | 7 | 5.83–8.15 | 0.63±0.05 | 0.500 | 1.04±0.05 |
| (0 1 3) | 0.1505 | 5 | 3.81–5.44 | 0.63±0.04 | 0.500 | 1.04±0.04 |
| (0 1 5) | 0.2196 | 10 | 2.64–3.59 | 0.65±0.04 | 0.500 | 1.06±0.04 |
| (0 1 7) | 0.2943 | 11 | 2.03–2.78 | 0.49±0.08 | 0.500 | 0.91±0.08 |
| (0 1 9) | 0.3712 | 7 | 1.58–2.17 | 0.23±0.05 | 0.500 | 0.63±0.07 |
| (0 3 1) | 0.2755 | 7 | 2.11–2.97 | 0.65±0.04 | 0.500 | 1.06±0.04 |
| (0 3 3) | 0.2979 | 7 | 1.94–2.73 | 0.40±0.05 | 0.500 | 0.83±0.06 |
| (0 3 5) | 0.3381 | 6 | 1.69–2.32 | 0.37±0.04 | 0.500 | 0.79±0.05 |
| (0 3 7) | 0.3907 | 3 | 1.70–2.00 | 0.41±0.09 | 0.500 | 0.83±0.10 |
| (1 2 0) | 0.2032 | 8 | 2.95–3.99 | 0.55±0.06 | 0.400 | 1.09±0.06 |
| (3 2 0) | 0.3277 | 3 | 1.97–2.50 | 0.18±0.03 | 0.154 | 0.99±0.08 |
| (1 4 0) | 0.3747 | 10 | 1.55–2.16 | 0.26±0.04 | 0.471 | 0.69±0.06 |
| (0 5 1) | 0.4561 | 7 | 1.29–1.73 | 0.25±0.05 | 0.500 | 0.65±0.08 |
| (0 5 3) | 0.4699 | 3 | 1.63–1.75 | 0.16±0.05 | 0.500 | 0.52±0.09 |
| (1 0 2)[a] | 0.1211 | 4 | 5.01–6.47 | 0.28±0.05 | 0.219 | 1.04±0.09 |
| (1 4 2)[a] | 0.3831 | 13 | 1.57–2.06 | 0.34±0.08 | 0.472 | 0.79±0.08 |

[a]These two reflections are obtained by subtracting the nuclear intensities from the total observed intensities and possibly subject to larger errors.

In this expression the magnetic scattering amplitude $p=\frac{1}{2}\gamma_0\mu f(\mathbf{Q})$, with $\gamma_0=0.539\times10^{-12}$ cm, $e^{-W}$ is the Debye-Waller factor, $\langle q\rangle$ is the magnitude of the magnetic interaction vector averaged over all magnetic domains, $\sigma_d=\pm1$, depending on the direction of the magnetic moment of atom $d$, and the sum in Eq. (1) is over the magnetic atoms located at position $\mathbf{r}_d$ in the magnetic unit cell. The Debye-Waller factor is not significantly different from unity in the $Q$ range covered in the present experiment. The magnetic scattering amplitudes $\mu f(\mathbf{Q})$ were calculated from Eq. (1) by assuming the spin structure (with two equally populated magnetic domains) described earlier in this section. The results of these calculations are listed in Table II.

## III. MAGNETIC FORM FACTOR AND MAGNETIZATION DENSITY

The experimentally determined magnetic scattering amplitudes $\mu f(\mathbf{Q})$ for $La_2NiO_4$ are compared with those of $La_2CuO_4$ in Fig. 4 for various values of $\sin\theta/\lambda$. For this comparison the $La_2CuO_4$ data were multiplied by a factor of 4 to account for the difference in the magnitude of the ordered moments of these compounds. It can be seen (Fig. 4) that the magnetic form factors of these compounds are quite similar and are characterized by a plateau at low $Q$ values. In addition, one cannot obtain a satisfactory fit to the data by using a simple ionic form factor. This can be seen by reference to Fig. 4, where the solid line is a least-squares fit to the $La_2NiO_4$ data using an ionic $Ni^{2+}$ $3d$ form factor.

To obtain some insight regarding the origin of the plateau in the measured form factor, we obtained the difference magnetization density by taking the Fourier transform of the observed density minus that obtained by fitting the data to an isotropic $Ni^{2+}$ $3d$ form factor. Series-termination errors were minimized by averaging the difference density over a box of dimensions $0.5\times0.5\times1.0$ Å$^3$.

Figure 5 shows the difference magnetization density map in the Ni-O plane. Here all Ni atoms at the corner positions have been defined to have positive density, represented by solid contours. Consequently, because of the antiferromagnetic ordering, the Ni atom at the face-center position has negative density, represented by dashed contours. Since this is a difference density map, there is little density near the Ni atoms. The main feature of this map is the appearance in the Ni-O plane of *antiparallel* densities around each Ni site. These densities are spread along the Ni-O bonds and disappear at the in-

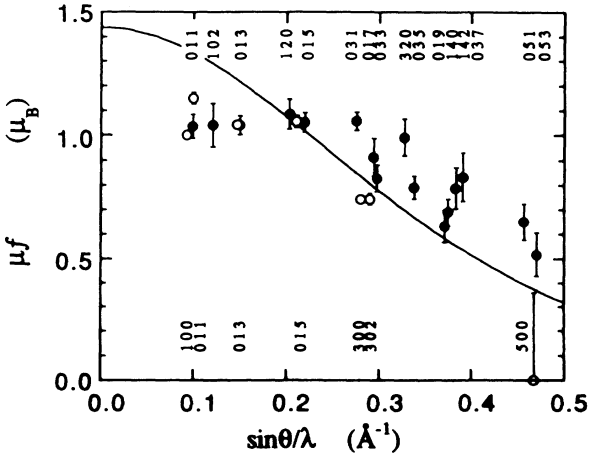


FIG. 4. $La_2NiO_4$ measured magnetic scattering amplitude vs $\sin\theta/\lambda$ (solid circles). For comparison, the experimental data (Ref. 2) for $La_2CuO_4$ (scaled by a factor of 4) are also plotted (open circles). The solid curve is a fit using an ionic $Ni^{2+}$ form factor.

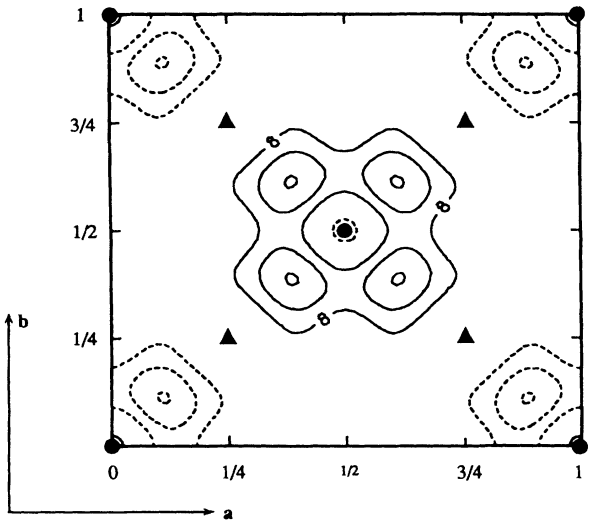


FIG. 5. Difference magnetization density in the Ni-O plane (see text). The atom symbols are circles, Ni; triangles, O. The solid and dashed contours denote positive and negative densities, respectively. Each contour is $8\times10^{-3}\mu_B/\text{Å}^3$. The Ni atoms at the corner positions have been defined to have positive densities.

plane oxygen sites, because the oxygen is midway between a positive and a negative Ni spin. Difference maps in other planes reveal no additional density above the significance level, which is about one contour ($8\times10^{-3}\mu_B/\text{Å}^3$) in Fig. 5. As a result, the magnetization density corresponding to the data is strongly anisotropic and, in particular, is contracted along the Ni-O bonds in the Ni-O plane. These observations suggest that the anomalous features of the magnetic form factor may be attributed to covalency effects[11–13] in the Ni-O plane. Such effects were found[12,13] to be of significance in many other transition-metal compounds, such as NiO and $K_2CuF_4$.

## IV. MODELING AND BAND CALCULATIONS

To assess the importance of covalency effects, we first adopted a very simple model where we assumed that the $Ni^{2+}$ unpaired electrons occupy an *isotropic orbital* with a radial dependence characteristic of the $Ni^{2+}$ $3d$ electrons. In the absence of any covalency effects, the magnetic form factor would be simply the isotropic $Ni^{2+}$ $3d$ ionic form factor. The effects of covalency were introduced by writing the electronic wave function as an antibonding mixture of the $Ni^{2+}$ $3d$ wave function with the O $2p_\alpha$ ($\alpha=x,y,z$) orbitals,

$$\Psi(\mathbf{r})=N\{d(\mathbf{r})+A^{\parallel}[p_x(\mathbf{r}-x_0\mathbf{i})-p_x(\mathbf{r}+x_0\mathbf{i}) +p_y(\mathbf{r}-y_0\mathbf{j})-p_y(\mathbf{r}+y_0\mathbf{j})] +A^{\perp}[p_z(\mathbf{r}-z_0\mathbf{k})-p_z(\mathbf{r}+z_0\mathbf{k})]\}\ , \quad (2)$$

where $N$ is a normalization constant, and $A^{\parallel}$, $A^{\perp}$ are the mixing parameters for the in- and out-of-plane oxygen atoms, respectively. In addition to the isotropic $3d$ distribution, the spin density contains two other terms: one due to the *d-p* overlap and the other arising from the spin density induced on the oxygen sites by covalency. The *d-p* overlap density is negative and can account for the plateau in the magnetic scattering amplitude at low $Q$ values. The induced spin density on the out-of-plane oxygen sites is positive and of O $2p$ character and contributes only to the innermost magnetic reflections, since it is much more spatially extended than the Ni $3d$ density. It should be noted, however, that for this antiferromagnetic compound, the induced moments on the in-plane oxygen atoms cancel out.

The model contains three parameters: the moment $m$ of a Ni ion in the absence of covalency effects and two mixing parameters $A^{\parallel}$ and $A^{\perp}$ for the in- and out-of-plane oxygen atoms, respectively. As can be seen from Fig. 6, we obtained with this model an excellent fit to the experimental data ($\chi^2$ was reduced from 10.7 to 1.7). Since $A^{\parallel}$ is much larger than $A^{\perp}$, this oversimplified model suggests that covalency effects involving primarily the in-plane rather than the out-of-plane oxygen atoms can account for the experimental observations. Since the induced moments on the in-plane oxygen atoms cancel out, the ordered moment $\mu$ is considerably reduced from its value $m$ attained in the absence of any covalency effects. In the present case, the ordered moment is $\mu=1.03\mu_B$, a reduction of nearly 50% from its expected value of $2\mu_B$. The model parameters are listed in Table III.

In the above analysis, we neglected the effects of the crystalline field on the $Ni^{2+}$ ion, which is in a crystalline field of tetragonal symmetry; its unpaired electrons are distributed between $d_{x^2-y^2}$ and $d_{3z^2-r^2}$ orbitals. As a result, the $Ni^{2+}$ form factor is anisotropic, the anisotropy depending on the relative population of the $d_{x^2-y^2}$ and $d_{3z^2-r^2}$ orbitals. The fit to the data using this form factor is, however, only marginally better than the one obtained using the $Ni^{2+}$ $3d$ form factor ($\chi^2$ is reduced from 10.7 to 9.9).

To assess the effect of covalency in this case, we form antibonding wave functions of the $d_{x^2-y^2}$ and $d_{3z^2-r^2}$ orbitals combined with O $2p_\alpha$ ($\alpha=x,y,z$) orbitals, noting

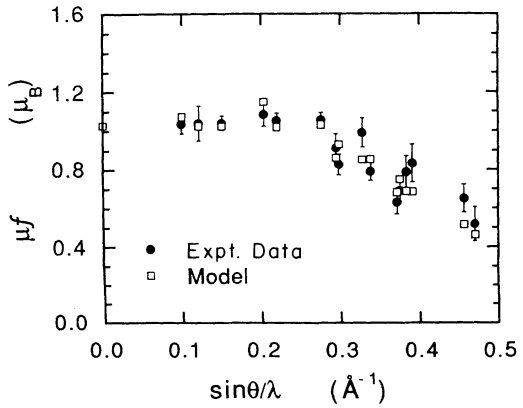


FIG. 6. Least-squares fit to the experimental data using a covalency model of a single antibonding orbital constructed from a spherical Ni $3d$ mixed with O $2p_\alpha$ ($\alpha=x,y,x$) orbitals.

that for the $d_{x^2-y^2}$ orbital only the in-plane oxygen atoms need to be included. The model contains five parameters: the moments $m_{x^2-y^2}$ and $m_{3z^2-r^2}$ and three mixing parameters $A_{x^2-y^2}$, $A^{\parallel}_{3z^2-r^2}$, and $A^{\perp}_{3z^2-r^2}$. In fitting the experimental data, various constraints were imposed to limit the number of parameters involved. In all cases the fit to the experimental data improved over that obtained using a simple superposition of the $d_{x^2-y^2}$ and $d_{3z^2-r^2}$ orbitals. For instance, by imposing the constraint $m_{x^2-y^2}+m_{3z^2-r^2}=2.2\mu_B$, $\chi^2$ is reduced from 9.9 to 6.7. The results for this particular model are given in Table III and Fig. 7.

As a natural extension of the discussion, we used the covalency model to analyze the antiferromagnetic form factor data[2] for $La_2CuO_4$. In an ionic model, the $Cu^{2+}$ ion has a $d^9$ configuration with the only unpaired electron occupying the $d_{x^2-y^2}$ orbital. Thus the modeling is much simpler than in the Ni compound. As shown in Fig. 8, an excellent fit is obtained with the $d_{x^2-y^2}$ covalency model. The fit leads to a moment $m_{x^2-y^2}=(0.61\pm0.03)\mu_B$ and a mixing parameter $A_{x^2-y^2}=0.51\pm0.02$. The value of this mixing parameter is comparable to that obtained for the Ni compound and

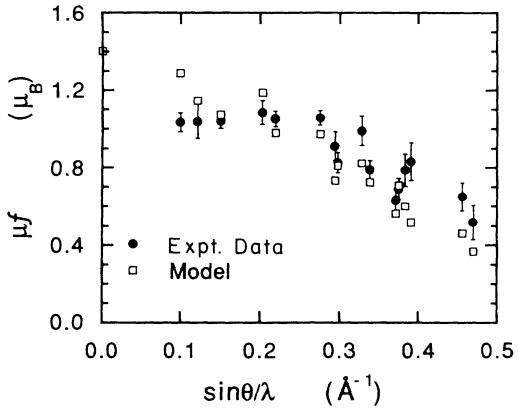


FIG. 7. Least-squares fit to the experimental data using a covalency model of two antibonding orbitals constructed, respectively, from a Ni $d_{x^2-y^2}$ and a $d_{3z^2-r^2}$ mixed with O $2p_\alpha$ ($\alpha=x,y,z$) orbitals.

is consistent with the results of paramagnetic band-structure calculations,[14(a)] which show that the states at the Fermi level have 40% Cu $d_{x^2-y^2}$ character. It is also consistent with the results of recent work,[14(b)] which extended the theory of covalence to include quantum spin

TABLE III. Least-squares fits to the experiment data of $La_2NiO_4$ with various models and band-theoretical calculations: (1) spherical 3*d*; (2) spherical 3*d* with covalency effects; (3) $d_{x^2-y^2}$ and $d_{3z^2-r^2}$ orbitals; (4) $d_{x^2-y^2}$ and $d_{3z^2-r^2}$ orbitals, including covalency effects, with the constraint $m_{x^2-y^2}+m_{3z^2-r^2}=2.2\mu_B$; (5) LAPW band calculations. The band result has been scaled by a factor 2.9, because the calculated moment is too small. Here *m* is the moment of a $Ni^{2+}$ ion in the absence of covalency effects, as compared with the net ordered moment $\mu$ predicted by the covalency models. The standard deviations of the fitting parameters are computed from the covariant matrix and may not reflect the actual confidence level of the fitting parameters.

| (*hkl*) | $\sin\theta/\lambda$ (Å$^{-1}$) | $\mu f(\mathbf{Q})$ ($\mu_B$) | (1) | (2) | (3) | (4) | (5) |
|---|---|---|---|---|---|---|---|
| (011) | 0.0993 | 1.04±0.05 | 1.33 | 1.08 | 1.34 | 1.29 | 1.38 |
| (013) | 0.1505 | 1.04±0.04 | 1.21 | 1.03 | 1.18 | 1.08 | 0.94 |
| (015) | 0.2196 | 1.06±0.04 | 1.01 | 1.02 | 0.94 | 0.98 | 1.03 |
| (017) | 0.2943 | 0.91±0.08 | 0.79 | 0.86 | 0.69 | 0.74 | 0.80 |
| (019) | 0.3712 | 0.63±0.07 | 0.58 | 0.69 | 0.49 | 0.56 | 0.51 |
| (031) | 0.2755 | 10.6±0.04 | 0.85 | 1.03 | 0.92 | 0.98 | 0.96 |
| (033) | 0.2979 | 0.83±0.06 | 0.78 | 0.93 | 0.80 | 0.81 | 0.62 |
| (035) | 0.3381 | 0.79±0.05 | 0.67 | 0.85 | 0.62 | 0.73 | 0.68 |
| (037) | 0.3907 | 0.83±0.10 | 0.54 | 0.69 | 0.43 | 0.52 | 0.51 |
| (120) | 0.2032 | 1.09±0.06 | 1.06 | 1.05 | 1.12 | 1.19 | 1.34 |
| (320) | 0.3277 | 0.99±0.08 | 0.70 | 0.85 | 0.82 | 0.82 | 0.98 |
| (140) | 0.3747 | 0.69±0.06 | 0.58 | 0.75 | 0.70 | 0.71 | 0.78 |
| (051) | 0.4561 | 0.65±0.08 | 0.40 | 0.52 | 0.52 | 0.46 | 0.50 |
| (053) | 0.4699 | 0.52±0.09 | 0.37 | 0.46 | 0.45 | 0.37 | 0.32 |
| (102) | 0.1211 | 1.04±0.09 | 1.29 | 1.03 | 1.27 | 1.15 | 1.08 |
| (141) | 0.3831 | 0.79±0.08 | 0.56 | 0.69 | 0.65 | 0.60 | 0.56 |
| | Reduced $\chi^2$ | | 10.7 | 1.7 | 9.9 | 6.7 | 9.3 |
| | Mixing parameter *A* | | | $A^{\parallel}=0.34\pm0.03$<br>$A^{\perp}=0.13\pm0.04$ | | $A_{x^2-y^2}=0.55\pm0.11$<br>$A^{\perp}_{3z^2-r^2}=0.28\pm0.05$<br>$A^{\parallel}_{3z^2-r^2}=0.13\pm0.15$ | |
| | Moment *m* ($\mu_B$) | | | $m=1.97\pm0.13$ | | $m_{3z^2-r^2}=1.01\pm0.09$<br>$m_{x^2-y^2}=1.19$ | |
| | Net ordered moment $\mu$ ($\mu_B$) | | | | $\mu_{x^2-y^2}=0.35$<br>$\mu_{3z^2-r^2}=1.08$ | $\mu_{x^2-y^2}=0.45$<br>$\mu_{3z^2-r^2}=0.95$ | $\mu_{x^2-y^2}=0.52$<br>$\mu_{3z^2-r^2}=0.78$ |
| | | | $\mu=1.44$ | $\mu=1.03$ | $\mu=1.43$ | $\mu=1.40$ | $\mu=1.38$ |

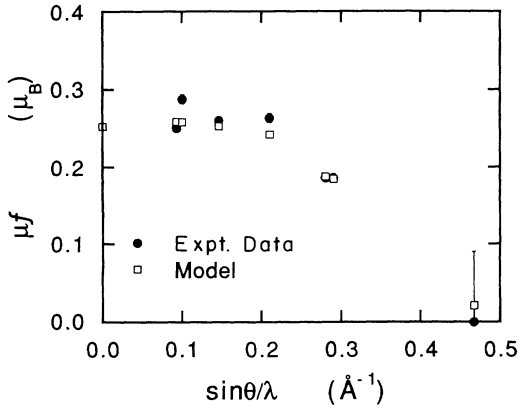


FIG. 8. Least-squares fit to the experimental data (Ref. 2) of $La_2CuO_4$ using a covalency model of a single antibonding orbital constructed from a Cu $d_{x^2-y^2}$ mixed with O $2p_\alpha$ ($\alpha=x,y$) orbitals.

fluctuations ( $A_{x^2-y^2}$ was found there to be between 0.35 and 0.45). A slight adjustment of the parameters also yields a good fit to the experimental data of the $Sr_2CuO_2Cl_2$ compound. The ordered moment computed from the fit to the $La_2CuO_4$ data is $\mu=0.25\mu_B$. Thus, in this model, covalency effects reduce the moment from $m_{x^2-y^2}=0.61\mu_B$ to $0.25\mu_B$. The value $\mu=0.25\mu_B$ is, within experimental error, the value obtained by Freltoft *et al.*[2] by fitting their data to a $K_2CuF_4$ form factor. These data were obtained for a sample with $T_N=185$ K. Values of $T_N$ and $\mu$ ranging up to 300 K and $0.6\mu_B$, respectively, were obtained with samples of different stoichiometry.[4,15,16] The values obtained by Freltoft *et al.* and in our analysis are consistent with that expected[4] for a sample with $T_N=185$ K.

The above models demonstrate that the magnetization density about the Ni sites deviates from that expected for an isotropic $Ni^{2+}$ ion. However, the models are rudimentary. While this simplifies the quantitative analysis, one should question the effects of the approximations of the models. For example, the antibonding phase relationship chosen between Cu and O orbitals is strictly only valid for states at the $X$ point in the Brillouin zone. Also, the radial part of the fitting functions was taken from free-ion calculations and clearly could be adopted to the environments in the solid to obtain a better fit.

To eliminate some of the arbitrariness, it would, of course, be desirable to perform first-principles calculations. For calculating spin densities in many magnetically ordered crystals, first-principles spin-polarized band-theoretical methods have proved very successful. However, in systems having strong intra-atomic Coulomb correlations, the usual density-functional approach is inadequate. For example, band theory is unable[14(a)] to stabilize the antiferromagnetic ground state of $La_2CuO_4$. For $La_2NiO_4$ an antiferromagnetic state is obtained,[17] whose moment is very sensitive to structural changes. To determine whether the magnetic ground state obtained from the first-principles spin-polarized band theory can provide any further insight into the measured form factor, we performed such calculations using the scalar relativistic linear augmented-plane-wave (LAPW) method. We used the exchange-correlation potential within the local-density approximation (LDA) specified by Moruzzi, Janak, and Williams.[18] The calculation did converge to an antiferromagnetic ground state, but with a moment of only $0.45\mu_B$ inside each Ni muffin-tin sphere. This is too small and reflects the problem with the LDA in treating the strong intra-atomic correlations. The band structure is very similar to that obtained by Guo and Timmerman,[17] and the large hybridization between $3d$ and $2p$ orbitals is similar to that obtained for $La_2CuO_4$.[14(a)] The large oxygen contribution to the antibonding bands near $E_F$ results in some contraction of the Ni spin density along the Ni-O bond direction, which is consistent with the picture inferred from the simple covalency models. Thus, in spite of the small moment, one might expect the basic shape of the electronic spin densities to be reasonably calculated. Indeed, by simply scaling the theoretical spin density by a factor of 2.9, a rather good fit to the experimental data is obtained (see Fig. 9).

The comparison between the experimental form factor and the one obtained from the band-structure calculation also suggests the kind of improvements that are needed for theories which go beyond band theory in treating the strong on-site correlation. The calculated anisotropy for the larger reflections agrees well with the experiment and arises from a 60%–40% contribution of states with Ni $d_{3z^2-r^2}$ and Ni $d_{x^2-y^2}$ character, respectively. We believe the reason that a larger moment is associated with the $d_{3z^2-r^2}$ orbital is that there is stronger covalent bonding between the $d_{x^2-y^2}$ and in-plane oxygen orbitals than for the $d_{3z^2-r^2}$ with the out-of-plane $p_z$ orbitals. The stronger bonding causes a greater bandwidth, and the magnetic interactions are less effective (a situation frequently encountered in itinerant magnetism). Although the anisotropy can be explained through covalency arguments, we believe the band structure overemphasizes the $d$-$p$ interactions. From model calculations using the three-band Hubbard Hamiltonian, it is clear that strong Coulomb correlations will reduce the effective hopping (or hybridization) between the $d$ and $p$ states.[19] At the same time, the magnetic moment is enhanced.

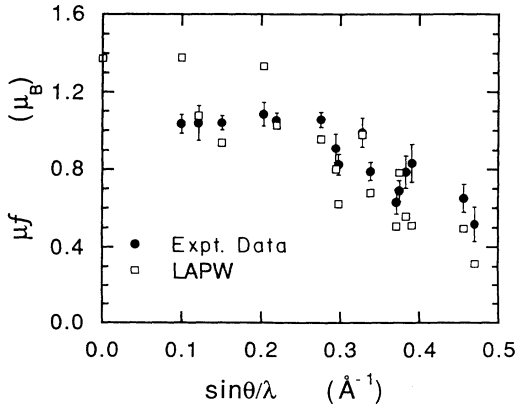


FIG. 9. Comparison with spin-polarized band calculations. The band result has been multiplied by a factor of 2.9 because the calculated moment is too small.

Besides the enhancement of the moment, which is clearly a problem for band theory, there are two other arguments which suggest that band theory seriously overestimates the *d-p* interactions. First, the larger discrepancy for the small reflections (Fig. 9) arises because the band theory yields a moment on the out-of-plane oxygens (about 10% of the moment on Ni). A correct treatment of the correlation would reduce both the *d-p* interaction and the oxygen moment relative to the Ni moment. The second evidence indicating that band theory overestimates the *d-p* hybridization derives from measurements of the induced magnetic form factor.[20,21] The induced form factor measures the response to a uniform applied field, and the in-plane oxygen may develop a moment. As discussed earlier, no moments exist on the in-plane oxygens in the antiferromagnetic form factor because of symmetry considerations Band theory suggests that the in-plane states near the Fermi level have as much as 60% oxygen *p* character and only 40% *d* character. The field-induced form-factor measurements, on the other hand, did not detect this oxygen character; however, because of the large experimental uncertainties, a small in-plane oxygen contribution cannot be excluded.[20,21]

Our experiments suggest that covalency effects may be contributing to the reduction of the ordered moment and thus raise the question of their importance relative to that of quantum spin fluctuations. Until recently, it was believed that quantum spin fluctuations could explain[4,15,16,22] the difference between the expected and observed moments in these compounds, without considering the effects of covalency. A recent three-band Hubbard model calculation incorporating both effects obtained a moment reduction of 17% as a result of covalency and another 18% as a result of spin fluctuations using parameters appropriate for $La_2CuO_4$.[19] However, until the difference between these theoretical results is resolved, it is difficult to make a detailed comparison with the experiments, especially since the neutron experiments measure the average moment, which, of course, depends on the stoichiometry of the samples. It is clear from the above discussion that there is need for experiments on stoichiometric samples, presumably those with the highest possible $T_N$, and further development of the theory to resolve these issues.

## V. SUMMARY

In summary, we have observed a pronounced plateau at low $Q$ in the antiferromagnetic form factor of $La_2NiO_4$. As a result, the observed $\mu f(\mathbf{Q})$ is poorly fitted by a spherical $Ni^{2+}$ $3d$ form factor. Nor can a good fit be obtained with the $d_{x^2-y^2}$ and $d_{3z^2-r^2}$ orbitals when crystal-field effects are taken into account. Similar results were obtained previously[2,3] for the cuprates $La_2CuO_4$ and $Sr_2CuO_2Cl_2$. The experimental results obtained in this experiment, as well as those[2,3] of $La_2CuO_4$ and $Sr_2CuO_2Cl_2$, were fitted to models in which we incorporated covalency effects. The results suggest that covalency effects in the Ni-O or Cu-O plane may be responsible for the plateau observed at low $Q$ values in the antiferromagnetic form factor of these compounds. We arrived at a similar conclusion from a comparison of the $La_2NiO_4$ data with first-principles spin-polarized band calculations, although the band-theoretical results seem to overemphasize the degree of *d-p* interaction.

## ACKNOWLEDGMENTS

We are especially grateful to S. K. Sinha and T. A. Kaplan for many helpful discussions. In addition we wish to thank P. Metcalf for her skillful technical work in the growth and annealing of the samples used in this study. Ames Laboratory is operated for the US DOE by Iowa State University under Contract No. W-7405-Eng-82. Work at Argonne is supported by the US DOE, BES–Material Science, Contract No. W-31-109-Eng-38. The Purdue research is supported by the Midwest Superconductivity Consortium through DOE Grant No. DE-FG02-90ER 45427.

[1]K. Yamada, K. Kakurai, Y. Endoh, T. R. Thurston, M. A. Kastner, R. J. Birgeneau, G. Shirane, Y. Hidaka, and T. Murakami, Phys. Rev. B **40**, 4557 (1989), and references cited therein; G. Aeppli, S. M. Hayden, H. A. Mook, S.-W. Cheong, D. Rytz, J. D. Remeika, G. P. Espinsosa, and A. S. Cooper, Phys. Rev. Lett. **62**, 2052 (1989); S. M. Hayden, G. Aeppli, H. A. Mook, S.-W. Cheong, and Z. Fisk, Phys. Rev. B **42**, 10 220 (1990).

[2]T. Freltoft, G. Shirane, S. Mitsuda, J. P. Remeika, and A. S. Cooper, Phys. Rev. B **37**, 127 (1988), and references cited therein.

[3]X. L. Wang, L. L. Miller, J. Ye, C. Stassis, B. N. Harmon, D. C. Johnston, A. J. Shultz, and C.-K. Loong, J. Appl. Phys. **67**, 4524 (1990).

[4]K. Yamada, E. Kudo, Y. Endoh, Y. Hidaka, M. Oda, M. Suzuki,, and T. Murakami, Solid State Commun. **64**, 753 (1987), and references cited therein.

[5]X. L. Wang, C. Stassis, D. C. Johnston, T. C. Leung, J. Ye, B. N. Harmon, G. H. Lander, A. J. Schultz, C.-K. Loong, and J. M. Honig, J. Appl. Phys. **69**, 4860 (1991).

[6]J. Rodríguez-Cavajal, J. L. Martínez, J. Pannetier, and R. Saez-Puche, Phys. Rev. B **38**, 7148 (1988).

[7]G. H. Lander, P. J. Brown, J. Spałek, and J. M. Honig, Phys. Rev. B **40**, 4463 (1989).

[8]Z. Kakol, J. Spałek, and J. M. Honig, Solid State Commun. **71**, 283 (1989).

[9]G. Aeppli and D. J. Buttrey, Phys. Rev. Lett. **61**, 203 (1988).

[10]K. Yamada, M. Matsuda, Y. Endoh, B. Keimer, R. J. Birgeneau, S. Onodera, J. Mizusaki, T. Matsuura, and G. Shirane, Phys. Rev. B **39**, 2336 (1989).

[11]J. Owen and J. H. M. Thornley, Rep. Prog. Phys. **29**, 675, (1966).

[12]W. Marshall and S. W. Lovesey, *Theory of Thermal Neutron Scattering* (Oxford University Press, New York, 1971), pp. 209–224.

[13]K. Hirakawa and H. Ikeda, Phys. Rev. Lett. **33**, 374 (1974).

[14(a)]T. C. Leung, X. W. Wang, and B. N. Harmon, Phys. Rev. B **37**, 384 (1988); 14(b) T. A. Kaplan, S. D. Mahanti, and Hyunju Chang, Phys. Rev. B **45**, 2565 (1992); T. A. Kaplan and S. D. Mahanti, J. Appl. Phys. **69**, 5382 (1991).

[15]Y. J. Uemura, W. J. Kossler, X. H. Yu, J. R. Kempton, H. E. Schone, D. Opie, C. E. Stronach, D. C. Johnston, M. S. Alvarez, and D. P. Goshorn, Phys. Rev. Lett. **59**, 1045 (1987).

[16]J. M. Tranquada, A. H. Moudden, A. I. Goldman, P. Zolliker, D. E. Cox, G. Shirane, S. K. Sinha, D. Vaknin, D. C. Johnston, M. S. Alvarez, A. J. Jacobson, J. T. Lewandowski, and J. M. Newsam, Phys. Rev. B **38**, 2477 (1988).

[17]G. Y. Guo and W. M. Timmerman, J. Phys. C **21**, L803 (1988).

[18]V. L. Moruzzi, J. F. Janak, and A. R. Williams, *Calculated Electronic Properties of Metals* (Pergamon, New York, 1978).

[19]T. C. Leung, Ph.D. thesis, Iowa State University, 1991.

[20]C. Stassis, B. N. Harmon, T. Freltoft, G. Shirane, S. K. Sinha, K. Yamada, Y. Endoh, Y. Hidaka, and T. Murakami, Phys. Rev. B **38**, 9291 (1988).

[21]G. H. Lander, P. J. Brown, C. Stassis, P. Gopalan, J. Spałek, and J. M. Honig, Phys. Rev. B **43**, 448 (1991).

[22]J. M. Tranquada and G. Shirane, Physica C **162-164**, 849 (1989).